JACS
JOURNAL OF THE AMERICAN CHEMICAL SOCIETY
Communication
pubs.acs.org/JACS

Arylazoindazole Photoswitches: Facile Synthesis and Functionalization via S_NAr Substitution

Raquel Travieso-Puente,[†] Simon Budzak,[‡] Juan Chen,[†] Peter Stacko,[†] Johann T. B. H. Jastrzebski,[§] Denis Jacquemin,*[,‡,⊥] and Edwin Otten*[,†]

[†]Stratingh Institute for Chemistry, University of Groningen, Nijenborgh 4, 9747 AG Groningen, The Netherlands
[‡]Laboratoire CEISAM - UMR CNRS 6230, Université de Nantes, 2 Rue de la Houssinière, BP 92208, 44322 Nantes Cedex 3, France
[§]Organic Chemistry & Catalysis, Debye Institute for Nanomaterials Science, Utrecht University, Universiteitsweg 99, 3584 CG Utrecht, The Netherlands
[⊥]Institut Universitaire de France, 1, rue Descartes, 75005 Paris Cedex 5, France

Supporting Information

ABSTRACT: A straightforward synthetic route to arylazoindazoles via nucleophilic aromatic substitution is presented. Upon deprotonation of the NH group, a C_6F_5-substituted formazan undergoes facile cyclization as a result of intermolecular nucleophilic substitution (S_NAr). This new class of azo photoswitches containing an indazole five-membered heterocycle shows photochemical isomerization with high fatigue resistance. In addition, the *Z*-isomers have long thermal half-lives in the dark of up to several days at room temperature. The fluorinated indazole group offers a handle for further functionalization and tuning of its properties, as it is shown to be susceptible to a subsequent, highly selective nucleophilic displacement reaction.

Photoswitchable organic compounds are of fundamental importance for applications ranging from data storage[1] and catalysis[2] to molecular biology[3] and photopharmacology.[4] Of the several classes of photoswitches that have been studied, those based on azobenzenes are popular due to their synthetic versatility and desirable properties, including large geometrical changes accompanying isomerization, high quantum yields, and fatigue resistance.[5] Azobenzene (PhN═NPh) shows a planar conformation in the most stable *E*-isomer; photochemical isomerization upon irradiation with UV light ($\pi\rightarrow\pi^*$ transition) leads to a photostationary state (PSS) that predominantly contains the *Z*-isomer. This isomer is unstable and reverts to the *E*-isomer either thermally or with irradiation in the visible range of the spectrum ($n\rightarrow\pi^*$ transition). Due to overlap between the absorption spectra of the two isomers, the visible irradiation often leads to incomplete conversion. While a large variety of substituted azobenzenes have been prepared to tune the (photo)chemical properties, these systems often suffer from low thermal stability of the *Z* isomer. This is problematic for applications such as optical data storage.[1a] Recently, substituted azobenzenes have been reported that combine significantly higher thermal stability with excellent photoswitching.[6] In contrast, heterocyclic analogues of azobenzenes have been so far largely ignored. Some examples of azopyridines[7] and azoimidazoles[8] were reported to behave as photodissociable ligands, leading to changes in spin state upon photoisomerisation of metal porphyrins bearing these ligands.[9] Fuchter et al. recently reported arylazopyrrole and arylazopyrazole photoswitches, which in some cases show long thermal half-lives and quantitative $Z\rightarrow E$ photoswitching.[10] Related arylazopyrazoles were used by Ravoo et al. in switchable supramolecular host–guest systems.[11] Although several methods have been reported for the synthesis of (substituted) azobenzenes,[12] high-yielding entries into new classes of azoheterocycles are desirable. Here we report a novel method that leads to the formation of photoswitches containing a (fluorinated) indazole as the 5-membered heterocycle. This type of azo-heteroaromatic structure was heretofore not considered for azo-containing photoswitches. The azo moiety is installed via a standard diazonium coupling to give a formazan derivative containing a C_6F_5 group. In a subsequent step, base-induced nucleophilic aromatic substitution[13] is used to form the indazole heterocycle in excellent overall yield (94%). The resulting arylazoindazoles show good switching behavior and cleanly undergo a subsequent S_NAr reaction to afford substituted derivatives.

Scheme 1. Synthesis of Azoindazoles 2 and 3

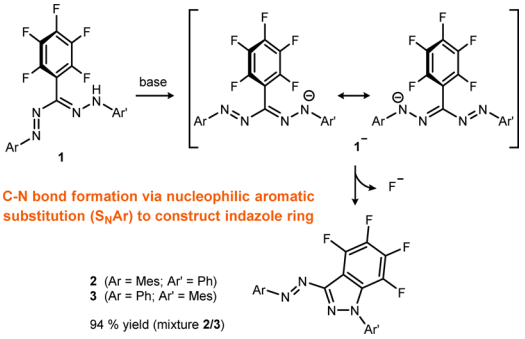

Treatment of formazan **1**[14] with 1.5 equiv of potassium hydride in THF resulted in deprotonation and subsequent nucleophilic aromatic substitution to release KF and to form the products **2** and **3** (Scheme 1), which were isolated as a mixture in 94% yield.[15] Analysis of these products by ^{19}F NMR spectros-

Received: December 14, 2016
Published: February 20, 2017

DOI: 10.1021/jacs.6b12585
J. Am. Chem. Soc. 2017, 139, 3328–3331

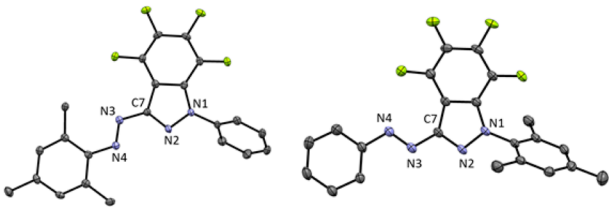

Figure 1. Molecular structures of **2** (left) and **3** (right) showing 50% probability ellipsoids (hydrogen atoms omitted for clarity).

copy indicated that the **2**:**3** ratio is ca. 1.45:1.00. Both compounds are shown by NMR spectroscopy to contain a C_6F_4 moiety in addition to Ph and Mes groups. Thus, we assigned **2** and **3** to be regioisomeric indazole compounds that differ in the position of the Ph and Mes groups (Scheme 1). Separation of **2** and **3** was achieved based on their different solubility: pure **2** can be obtained in 51% yield by crystallization from toluene, in which **3** is significantly more soluble. Isolation of pure **3** from these reaction mixtures was cumbersome; however, **3** is the major product when Me_2Zn is used as the base: the bis(formazanate)zinc complex formed upon treatment of 2 equiv of **1** with Me_2Zn cleanly undergoes an S_NAr reaction at 130 °C, giving **3** as the main product (**2**:**3** = 0.04:1) in 54% yield.[16]

Recrystallization of **2** and **3** afforded crystals that were suitable for X-ray diffraction (XRD) analysis. The atom connectivity observed in the solid state structures (Figure 1) confirms the products are formed by nucleophilic attack of the NAr moiety onto the C_6F_5 ring in the starting material. In these crystals, **2** and **3** have an *E*-configured N═N bond, but they differ in the orientation around the N(3)−C(7) bond (synperiplanar in **2**, antiperiplanar in **3**). Further evidence of the identity of **2** and **3** was obtained from $^1H-^{19}F$ correlation NMR spectroscopy (see the Supporting Information (SI)).

The azoindazoles **2**/**3** belong to the class of azoheteroarenes and are similar to the azoimidazoles[8] and azopyrroles/azopyrazoles[10a] that were recently reported to be efficient photoswitches. Similarly, **2** and **3** show photochemical switching behavior. While no changes are observed in the dark, an NMR sample of the mixture (in C_6D_6 solution) kept under ambient light for several days shows formation of two new compounds. A mixture containing the four components was analyzed by GC/MS, which showed that all have the same mass (413.11 *m*/*z*), suggesting that photochemical isomerization is taking place. UV/vis spectroscopy of pure *E*-**2** in toluene shows a broad absorption at 355 nm and a weaker, very broad band around 457 nm, attributed to $\pi\rightarrow\pi^*$ and $n\rightarrow\pi^*$ transitions, respectively (Figure 2). Irradiation in the high-energy band (λ_{irr} = 365 nm) results in photochemical isomerization with formation of a PSS that consists of 80% of the *Z*-isomer (based on integration of the ^{19}F NMR resonances). The $\pi\rightarrow\pi^*$ transition in *Z*-**2** is blue-shifted by 36 nm with a reduction in extinction coefficient, while the $n\rightarrow\pi^*$ bands of the *Z*- and *E*-isomer overlap significantly. As a consequence, the reverse ($Z\rightarrow E$) photoswitching by irradiation at 420 nm results in a PSS that shows incomplete conversion (49% of *E*-**2**). For compound **3**, the *Z*-isomer likewise has a lower molar extinction coefficient and a blue-shifted $\pi\rightarrow\pi^*$ absorption band with respect to *E*-**3**. However, the larger shift (50 nm) leads to a more efficient photoisomerization (PSS at 365 nm: 92% *Z*-**3**). In addition, the absorptions for *Z*-**3** and *E*-**3** show more pronounced differences in the visible range, leading to a higher PSS upon irradiation at 420 nm (70% of *E*-**3**). The quantum yields for the photochemical reactions were determined as 0.16/0.11 ($E\rightarrow Z$; λ_{irr} = 355 nm) and 0.60/0.47 ($Z\rightarrow E$; λ_{irr} = 457 nm) for **2**/**3**, respectively (see the SI for details).

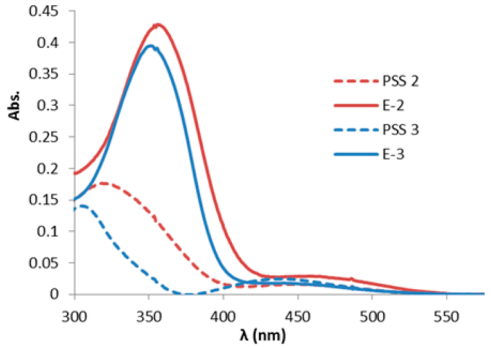

Figure 2. UV/vis spectra of *E*-**2** and *E*-**3** in toluene at 25 °C, and photostationary states (PSS) obtained upon irradiation of the samples at 365 nm (**2**, 80% *Z*-isomer; **3**, 92% *Z*-isomer).

The thermal stability of *Z*-**2** and *Z*-**3** was probed by monitoring the changes in the UV/vis spectrum at several temperatures between 60 and 105 °C in DMSO solution. A global fit of the kinetic traces afforded the activation parameters for the thermal $Z\rightarrow E$ isomerization as $\Delta H^{\ddagger}$ = 100.0 ± 1.3/96.9 ± 1.1 kJ/mol and $\Delta S^{\ddagger}$ = −24 ± 4/−21 ± 3 J·mol^{-1}·K^{-1} for **2**/**3**, respectively. These values extrapolate to free energies of activation at 25 °C of 107.1/103.3 kJ/mol and thermal half-lives of 7.7/1.6 days. High thermal stabilities are important for applications such as information storage, or *in vivo* uses. The slightly larger activation enthalpy for **2** (with the more hindered mesityl-subsituted azo moiety) is consistent with the notion that increasing the size of the *ortho*-substituents in azobenzenes leads to larger barriers.[17] For **2**, thermal isomerization kinetics were additionally measured in toluene to probe the influence of solvent polarity. These data lead to activation parameters ($\Delta H^{\ddagger}$ = 97.6 ± 1.6 kJ/mol and $\Delta S^{\ddagger}$ = −31 ± 5 J·mol^{-1}·K^{-1}) that are very similar to those in DMSO. The fatigue resistance of photochromic switches **2** and **3** was evaluated by repeating several isomerization cycles, which shows that they are robust: no photobleaching takes place (Figure 3), even upon irradiation over 20 days.

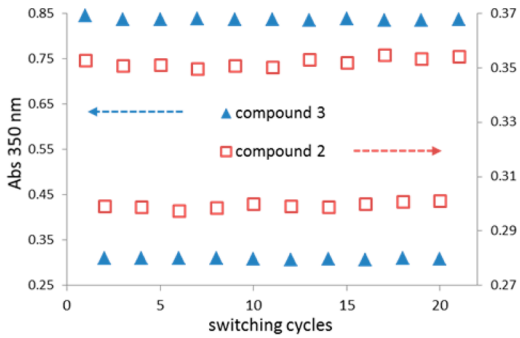

Figure 3. Switching cycles of **2** and **3** in DMSO, monitored by following the absorbance at λ = 350 nm, after irradiation at λ = 365 and 420 nm.

Aiming to take advantage of the susceptibility of the C_6F_4 ring toward further S_NAr substitution, we treated compound **2** with MeOH in the presence of NaOH (Scheme 2). Clean conversion to a single product was indicated by monitoring the reaction by ^{19}F NMR spectroscopy: three new resonances appeared in a 1:1:1 ratio, suggesting replacement of one F group by OMe (no further substitution takes place upon prolonged stirring under

DOI: 10.1021/jacs.6b12585
J. Am. Chem. Soc. 2017, 139, 3328−3331

Scheme 2. Synthesis of Functionalized Azoindazoles 4 and 5

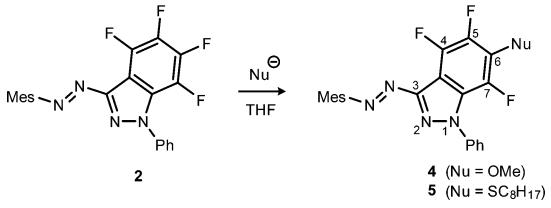

these conditions). On a preparative scale, the product was isolated in 80% yield. The ^{1}H NMR spectrum shows a singlet at δ 4.08 ppm integrating to 3H, diagnostic for the presence of an OMe group. The ^{19}F NMR resonances of the product appear as a triplet (δ −136.8 ppm) and two doublets (δ −148.5 and −158.3 ppm) which show similar F−F coupling constants of ∼20 Hz, in the range commonly found for either $^{3}J_{FF}$ (*ortho*) or $^{5}J_{FF}$ (*para*) coupling constants in fluoro-aromatics.[18] Similar to the starting material **2**, compound **4** shows H−F coupling between the Ph *o*-H group and a F substituent, suggesting that nucleophilic aromatic substitution does *not* take place at the site adjacent to the NPh group (the indazole 7-position). Homo- and heteronuclear (^{1}H,^{19}F) 2D NOE NMR experiments were used to unequivocally establish that **4** contains the OMe substituent on position C_6 of the indazole (see the SI). Similarly, the S-nucleophile *n*-octylthiolate reacted smoothly to give compound **5** (Scheme 2), but attempts to obtain addition of N-nucleophiles (NMR-scale reactions of **2** with deprotonated pyrrolidine or benzylamine in THF-d_8) did not result in clean substitution.[19]

The absorption maxima do not change appreciably upon going from **2** to **4**/**5**. Irradiation of *E*-**4** at 365 nm in C_6D_6 results in photochemical isomerization and formation of a PSS that consists of 75% of the *Z*-isomer of **4**. The back-reaction was monitored by irradiation at 420 nm and shown to result in the re-formation of 46% of *E*-**4**. Similar results are obtained for **5** (see the SI). Evaluation of the stability of *Z*-**4** in DMSO solution leads to similar activation parameters for the thermal *Z*/*E* isomerization as those found for the precursor **2** ($\Delta H^{\ddagger}$ = 99.2 ± 1.5 kJ/mol and $\Delta S^{\ddagger}$ = −26 ± 4 J·mol^{-1}·K^{-1}; half-life at 25 °C of 7.3 days). These data indicate that substitution of F for O- or S-alkyl groups does not significantly affect the photochemical and thermal switching behavior of this class of compounds. The facile nucleophilic aromatic substitution on compound **2** suggests that this reaction may present a more general strategy toward functionalized arylazoindazole photoswitches, for example for incorporation into biomolecular scaffolds[20] or attachment to surfaces.[21]

The flexible molecular skeletons of the compounds and the XRD study (see above) support the existence of several rotamers in addition to the two N═N bond isomers of azobenzene. Indeed, for the *E* isomer of each molecule, theoretical calculations lead to two rotamers that have similar energies (see the SI). Both *E* rotamers are separated by a relatively small barrier of ∼20 kJ/mol in the ground state, so their interconversion at room temperature should be facile. For the *Z* isomer, one of the rotamers (Z_2) is preferred by 14.2 kJ/mol, probably due to favorable C−H···π and CH_3···π interactions (see SI, Figure S25). As expected, the global energy minimum is the *E* isomer, which is ∼32 kJ/mol more stable than the *Z* form for **2**. This difference is smaller than in azobenzene, where we found a difference between *E* and *Z* as large as 54 kJ/mol at the same level of theory.

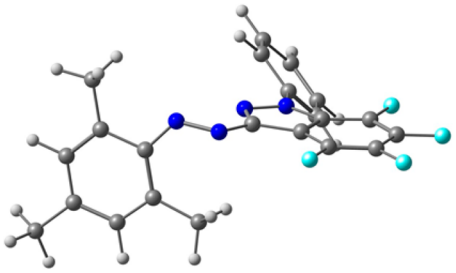

Figure 4. Calculated structure of the most accessible transition state for the thermal *Z*→*E* isomerization of **2**.

For azobenzene, rotation and inversion mechanisms are discussed in the literature as possible thermal reaction paths from *Z* to *E*.[22] Transition state calculations for **2** indicate that thermal *Z*→*E* isomerization follows the rotation pathway as this presents the lowest barrier, $\Delta G^{\ddagger}$ = 111 kJ/mol according to theory, in very good agreement with the experimental value of 107.1 kJ/mol (see Figure 4 for structure of the transition state). The inversion mechanism is slightly less favorable with $\Delta G^{\ddagger}$ = 124 kJ/mol. These DFT results agree well with CASPT2 calculations that provide activation energies of 137 kJ/mol (rotation) and 142 kJ/mol (indazole inversion). We underline that for **2**, DFT predicts a positive (negative) value of the activation entropy for the inversion (rotation) mechanism, further supporting that rotation is dominant (experimentally, $\Delta S^{\ddagger}$ is negative; see above). Similarly, the calculations for **3** and **4** indicate that the rotational pathway presents the lowest activation energies (see SI, Table S8). This contrasts with recent results for other azoheteroaryl switches where DFT calculations favored inversion.[10b]

Theoretical calculations reveal two low-lying excited-states for the *E* isomer which present n→π* (E-S_1) and π→π* (E-S_2) character in all molecules modeled. The n orbital is an out-of-phase combination of lone pairs on the two azo nitrogen atoms (SI, Figure S27). As the photoswitches are not perfectly planar, the first singlet excited-state has nonzero oscillator strength due to the admixture of π-orbitals from aromatic rings (TD-DFT: 468 nm, f = 0.06 for **2**). The second excited-state is strongly allowed (350 nm, f = 0.88 for **2**). The π and π* orbitals involved in the two lowest excited-states are bonding/antibonding orbitals centered mostly on N═N moiety (Figure S27). The vertical excitation energies of the different rotamers differ quite significantly (see SI, Table S9), and because their Boltzmann weights are comparable, both contribute to the experimentally measured broad UV/vis spectrum. The situation is slightly different for the *Z* isomer, where we found two n→π* excited-states with low oscillator strengths (for **2**, S_1: 479 nm, f = 0.04; S_2: 340 nm, f = 0.05) below the weak π(mesitylene)→π* excitation (S_3: 337 nm, f = 0.04) and a significantly dipole-allowed state (S_4: 328 nm f = 0.13). The two lowest excited-states have mostly n→π* character, comparable with *E*-S_1, while transitions in *Z*-S_3 involve orbitals combining the lone pairs from the azo nitrogen atoms and π orbitals from aromatic rings. In agreement with experiment, theory predicts a decrease of the oscillator strength for the allowed state when going from *E* to *Z*. The photochemical reaction inducing the *E*→*Z* conversion is initiated by high energy irradiation at 365 nm with population of the *E*-S_2 state. Assuming a behavior following Kasha's rules, S_2 rapidly relaxes to the S_1 state. On the S_1 potential energy surface of azobenzene, several structurally different S_1/S_0 conical intersections exist (following inversion/rotation motions),[23] and recent molecular dynamics studies of azobenzene and derived photoswitches found that

DOI: 10.1021/jacs.6b12585
J. Am. Chem. Soc. 2017, 139, 3328−3331

mostly rotational motion of the central N=N moiety brings the molecule toward a state-hopping geometry.[24] For the present compounds, the rotation around the N=N bond also brings the S_1 and S_0 states close to each other (−0.55 eV at CASPT2 level in TS_{rot} geometry), supporting a (photo)isomerization mechanism similar to the one found in "classical" azobenzene switches. Our calculations furthermore reveal that, in the lowest excited-state, the two *E* rotamers can reach a similar conical intersection by a barrierless path, whereas the excited-state interconversion between the two rotamers involves a small barrier (16 kJ/mol). As a result, the interconversion between the two rotamers in the excited state should be a minor process and should not strongly influence the observed quantum yields of photoconversion.[25]

In conclusion, we have developed a straightforward synthesis of arylazoindazoles via nucleophilic aromatic substitution. These compounds are shown to be photochromic switches that have moderate to high photoconversion in both directions, long thermal half-lives, and good fatigue resistance. These new azoindazoles could be useful as (switchable) bidentate ligands in coordination chemistry and catalysis, an avenue that we will pursue in future work. The possibility to further react the fluorinated ring with nucleophiles allows late-stage functionalization of this new class of photoswitches, potentially useful for their incorporation into biological scaffolds and functional materials.

■ ASSOCIATED CONTENT

Supporting Information

The Supporting Information is available free of charge on the ACS Publications website at DOI: 10.1021/jacs.6b12585.

X-ray crystallographic data for E-2 and E-3 (CIF)
Experimental procedures, NMR and UV/vis spectral data, and computational details (PDF)

■ AUTHOR INFORMATION

Corresponding Authors

*denis.jacquemin@univ-nantes.fr
*edwin.otten@rug.nl

ORCID

Denis Jacquemin: 0000-0002-4217-0708
Edwin Otten: 0000-0002-5905-5108

Notes

The authors declare no competing financial interest.

■ ACKNOWLEDGMENTS

The Netherlands Organisation for Scientific Research (NWO) is gratefully acknowledged for funding (VENI and VIDI grants to E.O.). We thank Pieter van der Meulen for assistance with ^{19}F NMR correlation spectroscopy and its interpretation, Prof. Ruud Scheek for help with Mathematica (fitting thermal isomerization data), and Prof. Wesley Browne for access to spectroscopic facilities and useful discussions. S.B. and D.J. acknowledge the support of the European Research Council (ERC - Marches 278845 grant). This research used computational resources of the CCIPL (*Centre de Calcul Intensif des Pays de Loire*), a local Troy cluster and French GENCI-CINES infrastructures.

■ REFERENCES

(1) (a) Irie, M.; Fukaminato, T.; Matsuda, K.; Kobatake, S. *Chem. Rev.* **2014**, *114*, 12174. (b) Zhang, J.; Zou, Q.; Tian, H. *Adv. Mater.* **2013**, *25*, 378.

(2) Göstl, R.; Senf, A.; Hecht, S. *Chem. Soc. Rev.* **2014**, *43*, 1982.

(3) Beharry, A. A.; Woolley, G. A. *Chem. Soc. Rev.* **2011**, *40*, 4422.

(4) (a) Velema, W. A.; Szymanski, W.; Feringa, B. L. *J. Am. Chem. Soc.* **2014**, *136*, 2178. (b) Broichhagen, J.; Frank, J. A.; Trauner, D. *Acc. Chem. Res.* **2015**, *48*, 1947.

(5) Bandara, H. M. D.; Burdette, S. C. *Chem. Soc. Rev.* **2012**, *41*, 1809.

(6) (a) Beharry, A. A.; Sadovski, O.; Woolley, G. A. *J. Am. Chem. Soc.* **2011**, *133*, 19684. (b) Bléger, D.; Schwarz, J.; Brouwer, A. M.; Hecht, S. *J. Am. Chem. Soc.* **2012**, *134*, 20597. (c) Samanta, S.; McCormick, T. M.; Schmidt, S. K.; Seferos, D. S.; Woolley, G. A. *Chem. Commun.* **2013**, *49*, 10314.

(7) (a) Otsuki, J.; Harada, K.; Araki, K. *Chem. Lett.* **1999**, *28*, 269. (b) Otsuki, J.; Narutaki, K.; Bakke, J. M. *Chem. Lett.* **2004**, *33*, 356. (c) Suwa, K.; Otsuki, J.; Goto, K. *Tetrahedron Lett.* **2009**, *50*, 2106.

(8) (a) Otsuki, J.; Suwa, K.; Narutaki, K.; Sinha, C.; Yoshikawa, I.; Araki, K. *J. Phys. Chem. A* **2005**, *109*, 8064. (b) Otsuki, J.; Suwa, K.; Sarker, K. K.; Sinha, C. *J. Phys. Chem. A* **2007**, *111*, 1403. (c) Wendler, T.; Schütt, C.; Näther, C.; Herges, R. *J. Org. Chem.* **2012**, *77*, 3284.

(9) (a) Venkataramani, S.; Jana, U.; Dommaschk, M.; Sönnichsen, F. D.; Tuczek, F.; Herges, R. *Science* **2011**, *331*, 445. (b) Thies, S.; Sell, H.; Schütt, C.; Bornholdt, C.; Näther, C.; Tuczek, F.; Herges, R. *J. Am. Chem. Soc.* **2011**, *133*, 16243. (c) Dommaschk, M.; Peters, M.; Gutzeit, F.; Schütt, C.; Näther, C.; Sönnichsen, F. D.; Tiwari, S.; Riedel, C.; Boretius, S.; Herges, R. *J. Am. Chem. Soc.* **2015**, *137*, 7552.

(10) (a) Weston, C. E.; Richardson, R. D.; Haycock, P. R.; White, A. J. P.; Fuchter, M. J. *J. Am. Chem. Soc.* **2014**, *136*, 11878. (b) Calbo, J.; Weston, C. E.; White, A. J. P.; Rzepa, H. S.; Contreras-García, J.; Fuchter, M. J. *J. Am. Chem. Soc.* **2017**, *139*, 1261.

(11) Stricker, L.; Fritz, E.-C.; Peterlechner, M.; Doltsinis, N. L.; Ravoo, B. J. *J. Am. Chem. Soc.* **2016**, *138*, 4547.

(12) (a) Merino, E. *Chem. Soc. Rev.* **2011**, *40*, 3835. (b) Konrad, D. B.; Frank, J. A.; Trauner, D. *Chem. - Eur. J.* **2016**, *22*, 4364. (c) Hansen, M. J.; Lerch, M. M.; Szymanski, W.; Feringa, B. L. *Angew. Chem., Int. Ed.* **2016**, *55*, 13514.

(13) (a) Vlasov, V. M. *J. Fluorine Chem.* **1993**, *61*, 193. (b) Vlasov, V. M. *Russ. Chem. Rev.* **2003**, *72*, 681.

(14) Chang, M. C.; Otten, E. *Chem. Commun.* **2014**, *50*, 7431.

(15) Ryabokon, I. G.; Polumbrik, O. M.; Markovskii, L. N. *Zh. Org. Khim.* **1983**, *19*, 230.

(16) A more detailed analysis of the influence of the base on the products obtained will be reported separately.

(17) (a) Nishimura, N.; Sueyoshi, T.; Yamanaka, H.; Imai, E.; Yamamoto, S.; Hasegawa, S. *Bull. Chem. Soc. Jpn.* **1976**, *49*, 1381. (b) Nishioka, H.; Liang, X.; Kashida, H.; Asanuma, H. *Chem. Commun.* **2007**, 4354. (c) Nishioka, H.; Liang, X.; Asanuma, H. *Chem. - Eur. J.* **2010**, *16*, 2054.

(18) Emsley, J. W.; Phillips, L.; Wray, V. *Prog. Nucl. Magn. Reson. Spectrosc.* **1976**, *10*, 83.

(19) Borch Jacobsen, C.; Meldal, M.; Diness, F. *Chem. - Eur. J.* **2017**, *23*, 846.

(20) (a) Hoppmann, C.; Maslennikov, I.; Choe, S.; Wang, L. *J. Am. Chem. Soc.* **2015**, *137*, 11218. (b) Mart, R. J.; Allemann, R. K. *Chem. Commun.* **2016**, *52*, 12262.

(21) (a) Russew, M.-M.; Hecht, S. *Adv. Mater.* **2010**, *22*, 3348. (b) Pathem, B. K.; Claridge, S. A.; Zheng, Y. B.; Weiss, P. S. *Annu. Rev. Phys. Chem.* **2013**, *64*, 605. (c) Klajn, R. *Pure Appl. Chem.* **2010**, *82*, 2247.

(22) (a) Cattaneo, P.; Persico, M. *Phys. Chem. Chem. Phys.* **1999**, *1*, 4739. (b) Cembran, A.; Bernardi, F.; Garavelli, M.; Gagliardi, L.; Orlandi, G. *J. Am. Chem. Soc.* **2004**, *126*, 3234.

(23) Yu, L.; Xu, C.; Zhu, C. *Phys. Chem. Chem. Phys.* **2015**, *17*, 17646.

(24) (a) Ciminelli, C.; Granucci, G.; Persico, M. *Chem. - Eur. J.* **2004**, *10*, 2327. (b) Shao, J.; Lei, Y.; Wen, Z.; Dou, Y.; Wang, Z. *J. Chem. Phys.* **2008**, *129*, 164111. (c) Pederzoli, M.; Pittner, J.; Barbatti, M.; Lischka, H. *J. Phys. Chem. A* **2011**, *115*, 11136. (d) Gámez, J. A.; Weingart, O.; Koslowski, A.; Thiel, W. *J. Chem. Theory Comput.* **2012**, *8*, 2352.

(25) (a) Wang, Y.-T.; Liu, X.-Y.; Cui, G.; Fang, W.-H.; Thiel, W. *Angew. Chem., Int. Ed.* **2016**, *55*, 14009. (b) See the SI for details.

DOI: 10.1021/jacs.6b12585
J. Am. Chem. Soc. 2017, 139, 3328−3331